

## THE STRUCTURE AND OPTICAL PROPERTIES OF CUPROUS TELLURIDE THIN FILMS

M. El-Bahrawy, S. Khodier, S. Kishk and N. Nagib  
National Institute for Standards, Cairo, Egypt

### Abstract

*The optical constants  $n(\lambda)$  and  $k(\lambda)$  of  $\text{Cu}_2\text{Te}$  thin films with thickness ranging from 12 to 69 nm deposited on glass substrates were determined from transmittance and near normal-incidence reflectance measurements in the wavelength range 400 – 2500 nm. The wavelength dependences of both  $n$  and  $k$  were found to have the same essential features for different thicknesses. Investigations of the structure of vacuum deposited  $\text{Cu}_2\text{Te}$  films by electron microscopy and X-ray diffraction showed the presence of two phases; the first and predominant is the hexagonal super structure with lattice parameters  $a_s = 1.268$  nm and  $c_s = 2.289$  nm while the second and less present is the face-centered cubic with  $a_s = 0.61$  nm.*

### Introduction

The structure of copper telluride has been studied by electron diffraction and X-ray [1-3] where it was found that thin films of  $\text{Cu}_2\text{Te}$  systems may be formed in amorphous or different crystalline states depending upon the conditions of preparation such as the type and temperature of the substrate. Sokol et al. [4] prepared  $\text{Cu}_2\text{Te}$  films by laser technique and studied the effect of annealing temperature on the film structure. They showed that annealing induced a hexagonal-cubic transition at  $T > 200^\circ\text{C}$ . Nikam [5] showed that the vapour phase deposited films of copper telluride on glass and rocksalt substrates at higher temperature exhibit five phases, which are tetragonal, normal hexagonal, hexagonal super structure, normal cubic ( $a_s = 0.635$  nm) and cubic super structure ( $a_s = 1.27$  nm). The most frequently appearing phases are the hexagonal and cubic. He

also obtained patterns corresponding to the phase  $\text{Cu}_2\text{Te}$  having tetragonal structure ( $a_p=0.398$ ,  $c_p = 0.612$  nm) at temperature up to  $200^\circ\text{C}$ . Baranova [6] studied the crystal structure of thin films of the hexagonal  $\beta^{\text{II}}$  phase of the Cu-Te system by electron diffraction and found the lattice parameters  $a_p = 0.417$  nm and  $c_p = 2.165$  nm.

On the other hand, no detailed studies of the optical properties of  $\text{Cu}_2\text{Te}$  thin films were carried out except those of Goswami and Rao [7]. They studied the optical properties of evaporated films of cuprous telluride and cuprous selenide in the visible region and reported that vacuum deposited films of  $\text{Cu}_2\text{Te}$  showed a semi-metallic behaviour as absorption was due to free charge carriers only.

The aim of the present work is to study the dependence of the structure of thin evaporated films of  $\text{Cu}_2\text{Te}$ , deposited on glass and carbon substrates on the film thickness. The optical constants  $n$  and  $k$  have been obtained in the wavelength range 400-2500 nm.

## 2. Experimental Procedure :

### 2.1 Preparation of the bulk material :

The cuprous telluride was prepared by fusion method at  $1200^\circ\text{C}$  of stoichiometric quantities of spec pure copper and tellurium (99.999%). Weighed quantities (taken to an accuracy of  $5 \times 10^{-4}$  g) contained in an evacuated sealed quartz ampule were heated in a two-section furnace, the hot end being kept at  $1200^\circ\text{C}$  while the cold end was kept at  $200^\circ\text{C}$  for 2 hrs. The temperature of the cold end was then raised gradually to  $700^\circ\text{C}$ , at which the synthesis took place. After the completion of the reaction, the temperature was raised to  $1200^\circ\text{C}$ . The product was left at that temperature for 5 hrs and continuous vibrational mixing was applied to homogenize the material. Then the ampoule was slowly cooled ( $50^\circ\text{C hr}^{-1}$ ) to  $800^\circ\text{C}$  and left for three days in order to ensure homogeneity, and finally the

current of the furnace was switched off and the ampule was left to cool down to room temperature.

An X-ray diffraction pattern of the prepared powder material is shown in Fig. (1). The interplaner spacings  $d$  (nm) were calculated and compared with the standard JCPDS data [8] for various Cu-Te systems. This analysis showed that the prepared powder material is mainly of the hexagonal  $\text{Cu}_7\text{Te}$  phase with a minor proportion of cubic  $\text{Cu}_7\text{Te}$  phase. The analysis also showed the presence of traces of  $\text{Cu}_{2-x}\text{Te}$  (tetragonal) and Te (hexagonal) phases.

## 2.2 Preparation of thin films :

Owing to the large difference in the melting points of copper and tellurium, several precautions according to, Farag and Khodier [9], have been taken during the preparation of thin films. The optimum conditions for vacuum-deposited films, confirmed by X-ray diffraction analysis were found to be close to those for flash evaporation (i.e., rapid evaporations of finely divided particles falling on a hot filament). Glass substrates maintained at room temperature ( $27^\circ\text{C}$ ) were found to be satisfactory, as it was found that the film adhered less well to the surface of the substrate at higher substrate temperature. X-ray diffraction analysis shows that low rates of evaporation ( $0.5 \text{ nm}\cdot\text{s}^{-1}$ ) decompose the compound. On the contrary, high rates ( $3\text{-}5 \text{ nm}\cdot\text{s}^{-1}$ ) reduce the decomposition of the compound and give homogeneous layers of the same constituents as the initial compound. On the basis of these optimum conditions, different film thicknesses ranging from 12 nm to 69 nm were thermally evaporated onto glass and carbon substrates in a vacuum of  $10^{-5}$  Torr ( $1.3 \times 10^{-3}$  Pa). Unannealed films are found to be amorphous as shown by X-ray diffraction [9]. Annealing of these films for 2 hrs at  $200^\circ\text{C}$  changes them to the crystalline state.

## 2.3 Film characterizations and measurements

Film thicknesses were determined to  $\pm 1.5$  nm by the method of

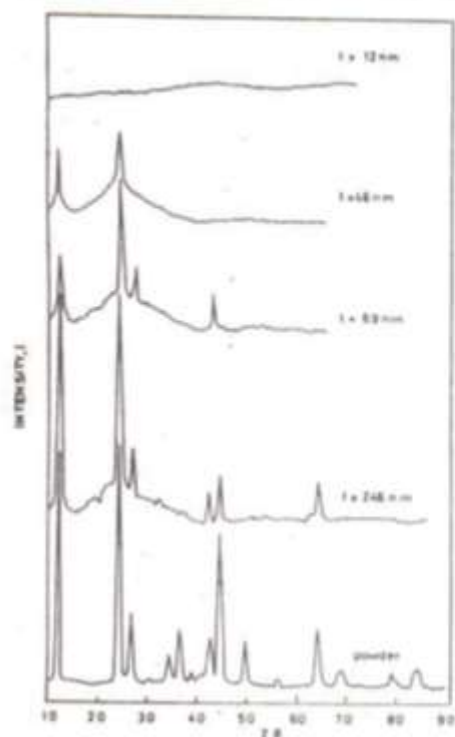


Fig. 1 X-ray diffraction patterns of powder and  $\text{Cu}_2\text{Te}$  films of thickness 12 nm, 46 nm, 69 nm, and 246 nm.

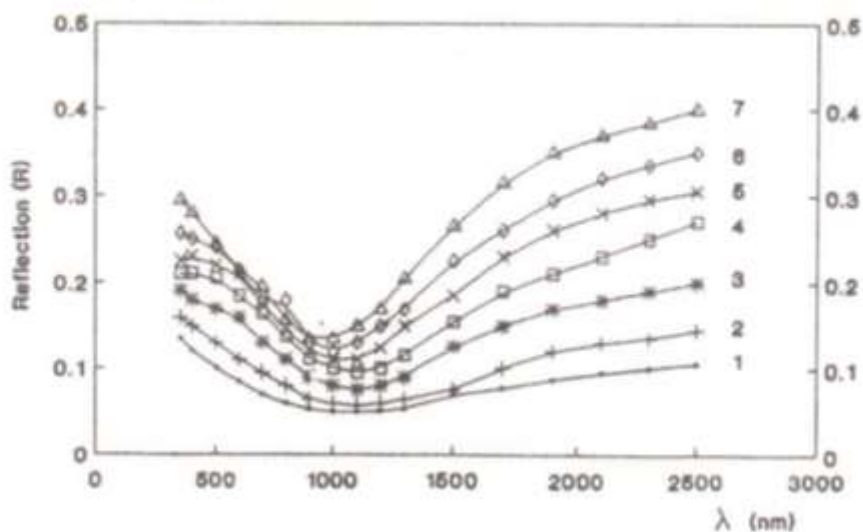


Fig. 2 Experimental variation of reflection with wavelength.



multiple beam interference at reflection described by Tolansky [10]. An X-ray diffractometer with copper target ( $\lambda = 0.154 \text{ nm}$ ) was used. The patterns were automatically recorded using rate meter time constant 250 pulse/second and scanning speed of  $2^\circ/\text{minute}$ . Transmission and diffraction investigations for films deposited on glass substrates were carried out using Electron Microscope (Zeiss (E.M./10) (100KV) with resolving power of 0.4 nm] for the films deposited on carbon substrates. Near normal incidence ( $7^\circ$ ), air/film reflectance  $R$  and normal incidence transmittance  $T$  were measured in the wavelength range from 400 nm to 2500 nm using a single-beam spectrophotometer (type PMQ3) with assembly attachment for specular reflection measurements [11]. Experimental  $R(\lambda)$  and  $T(\lambda)$  for seven films of different thicknesses are shown in figs. (2) and (3).  $R$  and  $T$  values were reproducible to  $\pm 1\%$ , and were used in the determination of the optical constants  $n$  and  $k$ .

### 3. RESULTS AND DISCUSSION

#### 3.1 The optical constants :

The theoretical expressions for the transmittance  $T$  and the reflectance  $R$ , at normal incidence on plane parallel absorbing film on a non-absorbing substrate are given as:

$$T = \frac{16 n_o n_g (n^2 + k^2)}{E e^{\beta} + F e^{-\beta} + 2G \cos \alpha + 4H \sin \alpha} \quad (1)$$

$$R = \frac{A e^{\beta} + B e^{-\beta} + 2C \cos \alpha + 4D \sin \alpha}{E e^{-\beta} + F e^{\beta} + 2G \cos \alpha + 4H \sin \alpha} \quad (2)$$

where  $n_o$  and  $n_g$  are the refractive indexes of the first medium (air) and the substrate (glass),  $\alpha = 4 \pi t n / \lambda$ ,  $\beta = 4 \pi t k / \lambda$  and  $t$  is the thickness of the film.  $A, B, \dots, H$  are functions of  $n$  and  $k$ . The mathematical expressions for these functions are given explicitly in [12]. Applying

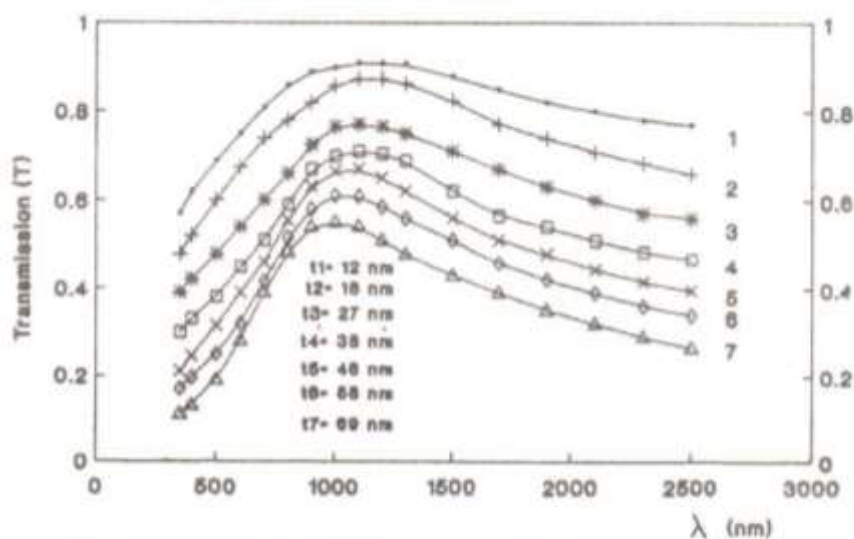


Fig. 3 Experimental variation of transmission with wavelength.

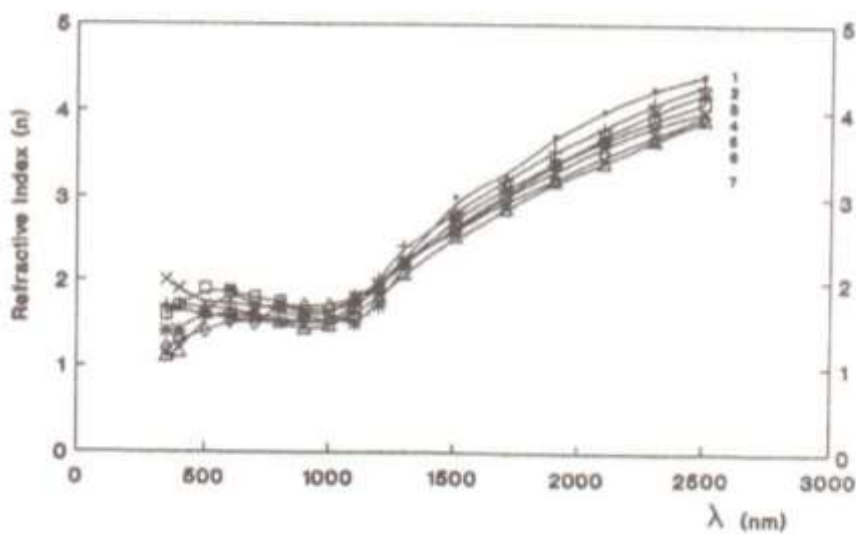


Fig. 4 The relation between the refractive index  $n$  and wavelength

Hadley's method [13,14], the measured quantities R and T were used in the determination of the refractive index  $n$  and the absorption index  $k$ . The procedure involves considerable computations. The overall uncertainty in  $n$  and  $k$  values for a particular value of  $t/\lambda$  was  $\pm 0.02$ .

The optical constants  $n(\lambda)$  and  $k(\lambda)$  for  $\text{Cu}_2\text{Te}$  thin films were determined and the curves exhibit the same trend, Figs. (4) and (5). It was found that the optical constants decrease gradually as the wavelength increases reaching minimum and then increase again. The essential feature of these curves is the presence of a minimum ( $n_{\min}$ ) and ( $k_{\min}$ ) between  $\lambda = 900$  nm and  $\lambda = 1200$  nm. Values of  $k_{\min}$  are also sensitive to the film thickness. In particular, this minimum position shifts to shorter wavelengths as the thickness increases. It is also clear from Figs. (4) and (5) that, above  $\lambda = 1500$  nm,  $n$  decreases with increasing film thickness while  $k$  increases as the thickness increases.

### 3.2 Structural properties :

It was found that, at the preliminary stage of a  $\text{Cu}_2\text{Te}$  deposited layer, the film consists of very small nuclei. Fig. (6) (a, b) shows the micrographs of  $\text{Cu}_2\text{Te}$  films of thickness 27 nm and 46 nm, respectively. The electron diffraction of these films possess polycrystalline structure. Figure (6) (e,f) shows patterns which composed of continuous rings; there are two strong bright diffused rings that remain essentially unchanged with film growth. By further increase of the film thickness, coalescence process leads to the formation of fine crystallites of larger sizes, shown in Fig. (6) (c,d) for films of thicknesses 56 nm and 69 nm respectively.. The corresponding electron diffraction patterns, Fig. (6) (g, h) show spots which was interpreted as initial steps of crystallization in films of higher thicknesses.

X-ray diffraction patterns of thin  $\text{Cu}_2\text{Te}$  films of thicknesses ranging from 12 nm to 69 nm are shown in Fig. (1). It is clear that

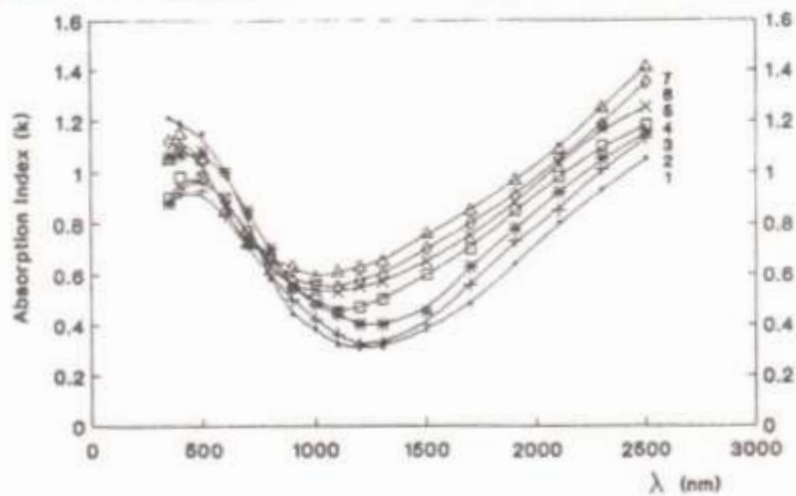


Fig. 5 The relation between the absorption index  $k$  and wavelength.

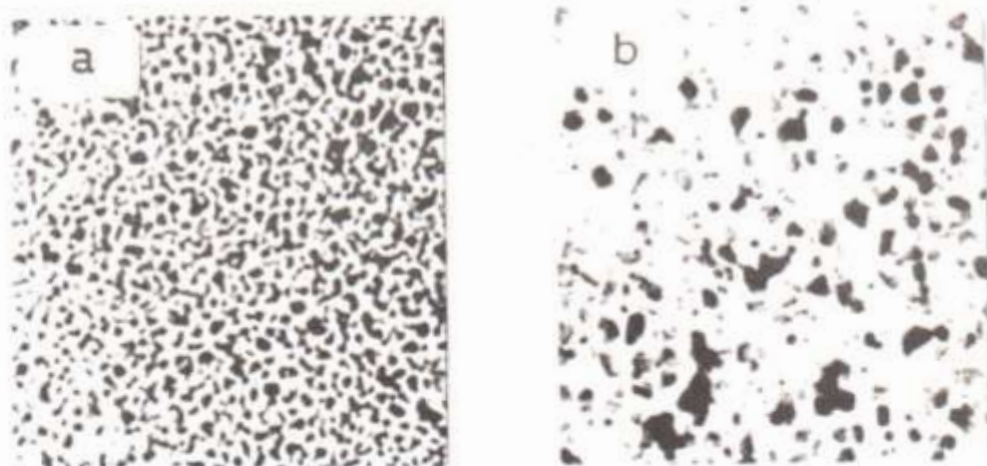


Fig. 6 Transmission electron micrographs and electron diffraction patterns:  
 (a, e)  $t = 27$  nm . (b, f)  $t = 46$  nm  
 (c, g)  $t = 56$  nm . (d, h)  $t = 69$  nm



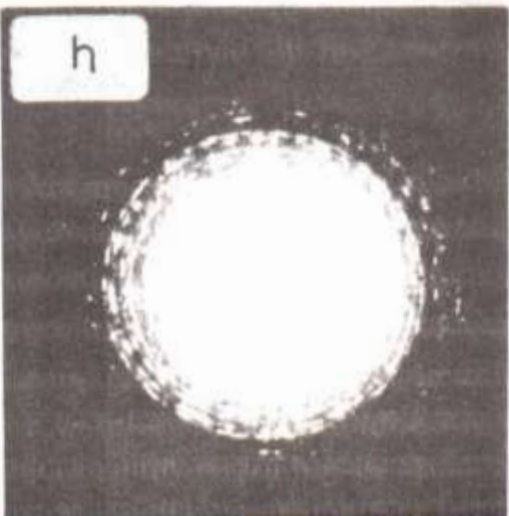
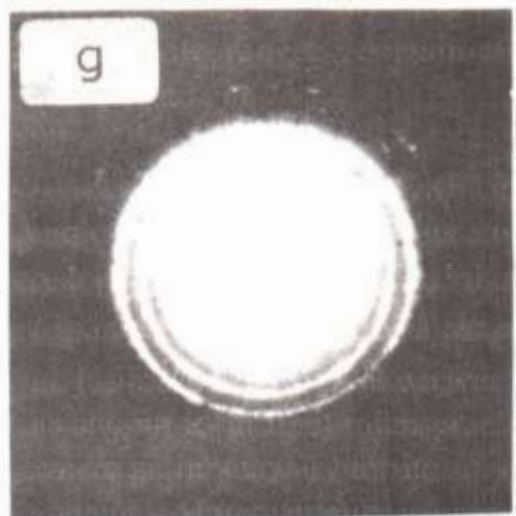
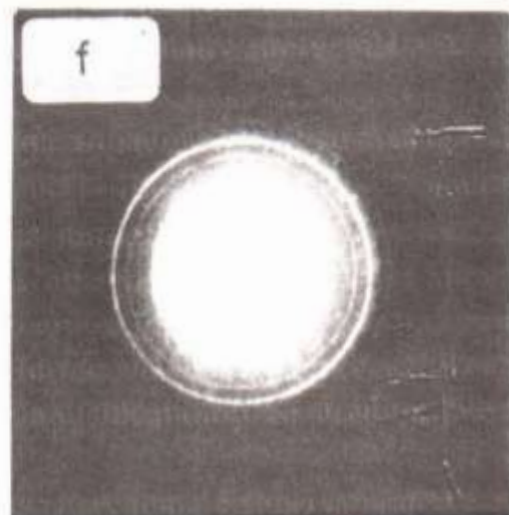
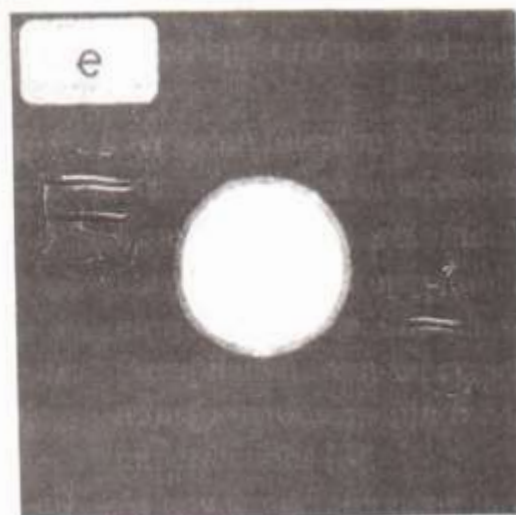
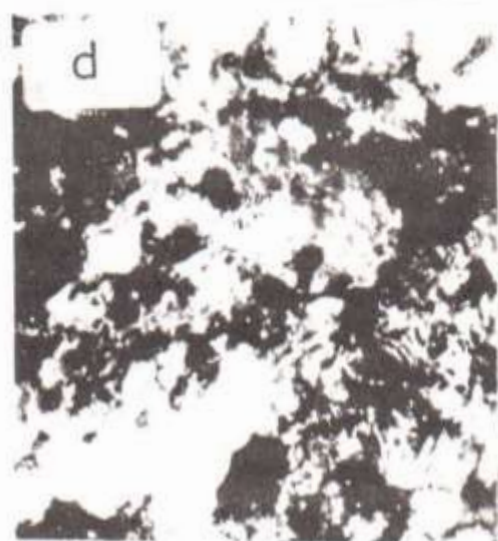
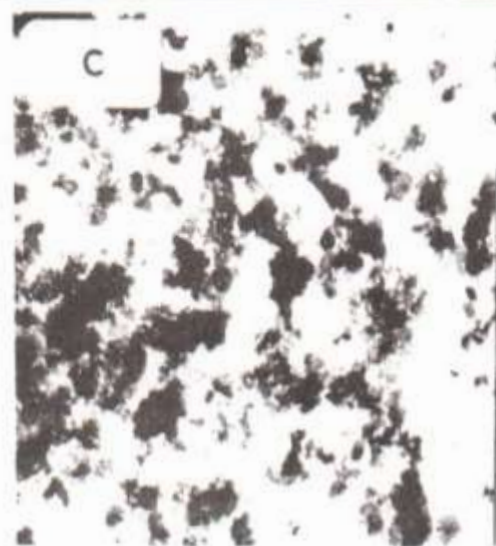
the peak heights increase as the film thickness increase with the appearance of new peaks for higher thicknesses. The peak heights corresponding to the reflection of the plane (300) or (006) can be taken as an indication for the increase of the degree of preferred orientation. The interplanar d-spacings were calculated for  $\text{Cu}_2\text{Te}$  thin films (27 nm) from the electron diffraction patterns and for powder and films of different thicknesses from X-ray diffraction patterns. The results are listed in tables (1) and (2), respectively.

It is apparent from tables (1), (2) and Fig. (1) that the structure of all films is predominantly of hexagonal super structure phase with feeble presence of F.C.C. phase. They also show that the preferred growth planes for the hexagonal phase are (003), (300), (006), (303), (330), (333) and (609) planes and for F.C.C. are (133) and (224) for  $\text{Cu}_2\text{Te}$  films.

The lattice parameters  $a_0$  and  $c_0$  of the film are determined from analysis of electron diffraction data (table 1) and were found to be for  $\text{Cu}_2\text{Te}$  hexagonal super structure :  $a_0 = 1.268$  nm and  $c_0 = 2.289$  nm. the F.C.C. phase of  $\text{Cu}_2\text{Te}$  has lattice constant  $a_0 = 0.61$  nm. These results are in good agreement with X-ray diffraction analysis of deposited bulk layer listed in table (2), and also with the previously published results [2-6].

#### 4. CONCLUSION

In the present study, it was found that the annealed  $\text{Cu}_2\text{Te}$  thin films have polycrystalline structure for the entire range of thicknesses from 27 to 69 nm. The crystallite size was found to increase with increasing film thickness. The structure of  $\text{Cu}_2\text{Te}$  films are predominately of hexagonal super structure and feeble presence of F.C.C. structure. The lattice parameters were found to be  $a_0 = 1.268$  nm,  $c_0 = 2.289$  nm for hexagonal super structure and  $a_0 = 0.61$  nm for cubic phases.



The optical constants  $n$  and  $k$  were determined in the range  $\lambda = 400 - 2500$  nm. As the hexagonal super structure is predominantly present in the films structure, it was concluded that the values of  $n$  and  $k$  are highly representatives of this phase. Above 1500 nm, both of the constants  $n$  and  $k$  increase monotonically with  $\lambda$  for all film thicknesses. The minima encountered in the values of  $k$  between 1000 and 1200 nm was found to be dependent on the film thickness. This dependence is such that as the thickness increases,  $k_{\min}$  shifts to lower  $\lambda$ -values. In relation to the structure, the optical constants of the film with highest thickness (69 nm) are the closest to the bulk material constants.

### References

1. G. P. Thomson, Proc. R. Soc. London (GB) 28, 649 (1930).
2. A. Goswami & S. P. Nikam, Indian J. Pure and Applied Phys., 8, 798 (1970).
3. A. Goswami & S.P. Nikam, J. Crystal Growth, 8, 247 (1971).
4. A. A. Sokol, V. M. Kosevich, A. D. Barvinok, Izv. Akad. Nauk. USSR, Neorg. Mater., 21, 1306 (1985).
5. S. P. Nikam, Indian J. of Pure and Applied Phys. 20, 654 (1982).
6. R.V. Baranova, Soviet Physcis-Crystallography, 13, 695 (1969).
7. A. Goswami, and B. V. Rao, Indian J. Phys., 50, 50 (1976).
8. I. C. P. d. S. International Centre for diffraction data powder diffraction file search manual, 7-106, 10-421, 4-836, 27-871, 18-1344, 4-554.
9. B. S. Farag, and S. A. Khodier, Thin Solid Films, 201, 231 (1991).
10. S. Tolansky, Multiple Beam Interferometry, Oxford University Press, London, 1948, m P. 149.
11. S. Khodeir, Ph. D. Thesis, Ain Shams University, Faculty of Science (1991).
12. D. Male, C. R. Acad., Sci., Paris, 230, 1349 (1950).
13. I. N. Hadley, and D. M. Dennison, J. Opt. Soc. Am, 37, 451 (1947).
14. A. El-Shazley and H.T. El-Shaer, Thin Solid Films, 78, 287 (1981).

Table (1)

Electron diffraction of thin  $\text{Cu}_2\text{Te}$  film (27 nm)

Obs. $I/I_0$	$d_{\text{obs}}$ (nm)	d (nm) ASTM Card			
		Te Hexagonal	Cu <sub>2</sub> Te Hexagonal hkl	Cu <sub>2</sub> Te F.C.C. hkl	Cu <sub>2-x</sub> Te Tetragonal
m	0.42437	0.4158			
v.s.	0.37755		0.361 (300) (006)		
m	0.31242		0.324 (303)		
w	0.24272				0.242
m	0.20276		0.201 (333)		
w	0.16700		0.162 (606,3012)		
w	0.15570		0.156 (441)		
m	0.13916			0.141 (133)	
v.w	0.13204		0.134 (3015)		
v.w	0.12002			0.123 (224)	

very weak (v.w.), weak (w), medium (m), strong (s), and very strong (v.s)



Table 2

Values of d-spacing and intensity of bulk and thin films of  $\text{Cu}_2\text{Te}$  by X-ray diffraction.

Powder form		Film thickness						ASTM card	
		46 (nm)		69 (nm)		246 (nm)			
d(nm)	$I/I_0$	d(nm)	$I/I_0$	d(nm)	$I/I_0$	d(nm)	$I/I_0$	d(nm)	Phase hkl
0.719	100	0.719	80	0.719	52.8	0.719	100	0.725	$\text{Cu}_2\text{Te}$ (003) hexa
0.36	100	0.360	100	0.360	100	0.360	100	0.361	$\text{Cu}_2\text{Te}$ (300,006)hexa
0.321	29			0.321	45	0.321	33	0.324	$\text{Cu}_2\text{Te}$ (303) hexa
0.255	11					0.255	9	0.255	$\text{Cu}_2\text{Te}$ (306) hexa
0.24	17					0.240	5	0.242	$\text{Cu}_{2-x}\text{Te}$
0.228	6							0.227	$\text{Cu}_2\text{Te}$ (218) hexa
0.217	5							0.217	$\text{Cu}_2\text{Te}$ (500,0010)hexa
0.207	26			0.207	28	0.207	14	0.209	$\text{Cu}_2\text{Te}$ (330) hexa
0.200	64					0.200	22	0.201	$\text{Cu}_2\text{Te}$ (333) hexa
0.179	18							0.176	$\text{Cu}_2\text{Te}$ (603) hexa
0.161	4							0.162	$\text{Cu}_2\text{Te}$ (606,3012)hexa
0.144	22					0.144	18	0.145	$\text{Cu}_2\text{Te}$ (609,0015)hexa
0.134	9							0.134	$\text{Cu}_2\text{Te}$ (3015)hexa
0.12	7							0.123	$\text{Cu}_2\text{Te}$ (224) F.C.C.
0.114	9							0.113	Te